Localization and shot noise in quantum nanostructures

(Invited Paper)

M. Macucci, P. Marconcini, and G. Iannaccone
Dipartimento di Ingegneria dell'Informazione
Università di Pisa
via Girolamo Caruso 16, I-56122 PISA, Italy
e-mail: macucci@mercurio.iet.unipi.it

***Abstract*—We present an investigation with a quantum model of shot noise suppression in a series of cascaded barriers, showing that the well-known diffusive limit reported in the literature on the basis of semiclassical models can be achieved only in the presence of a mechanism leading to mode mixing, such as a magnetic field. Without mode mixing, strong localization appears, because the localization length is of the order of the mean free path. These results are consistent with existing experimental data on shot noise in superlattices.**

I. Introduction

It is well known that in diffusive conductors the power spectral density of shot noise at low frequencies is suppressed down to 1/3 [1], [2] of the value $2qI$ (where q is the electron charge and I is the average current) predicted by Schottky's theorem [3] for uncorrelated carriers. This has also been experimentally demonstrated [4] for the case of disordered metallic conductors, where the conditions for diffusive transport are better achieved than in bulk semiconductors or in semiconductor nanostructures.

Therefore it is well-established that both from a semiclassical and from a quantum point of view systems characterized by 2-dimensional or 3-dimensional disorder can lead to a Fano factor (ratio of the actual noise power spectral density to that expected from Schottky's theorem) of 1/3, if proper conditions for the disorder strength and for the number of propagating modes are satisfied [5], [6].

There was a seminal paper by De Jong and Beenakker [7] that extended this result, within a semiclassical model, to a series of cascaded barriers, for which, independent of barrier transparency, a Fano factor of 1/3 was found. This result received also a numerical confirmation from a semiclassical Monte Carlo simulation [8].

This led to a somewhat generalized belief that the 1/3 suppression was to be expected also from the point of view of a quantum model and that 1-D disorder (represented by randomly spaced cascaded barriers) was substantially equivalent, from the point of view of shot noise suppression and of the onset of diffusive transport, to 2-D and 3-D disorder, for which a quantum model of shot noise leads to the same 1/3 suppression as the semiclassical one.

As a result, Song *et al.* [9], while measuring shot noise in a superlattice, were expecting to find a suppression down to 1/3, considering the large number of barriers, while they actually got values scattered over a rather wide range.

Indeed, a quantum calculation of the Fano factor for a series of cascaded barriers yields a result [10] that may appear surprising at first. The computed value does not converge to 1/3 as the number of barriers is increased, but, rather, takes on different values depending on barrier transparency, approaching unity in the case of opaque barriers. The reason behind this apparent contradiction is that all semiclassical models are based on the definition of a well defined occupancy in each region between two barriers, an occupancy that depends only on energy. In the presence of 1-D disorder (represented by the barriers) this is not possible, because there is no mixing between different transverse modes. The presence of a magnetic field does, however, introduce mode mixing, and, under proper conditions, can lead to the 1/3 shot noise suppression limit predicted by semiclassical theories. Here we focus specifically on the effect of magnetic field on shot noise and discuss the conditions for which the diffusive limit may be retrieved. An equivalent approach to the physical system we are considering is in terms of localization length: in the presence of mode mixing, the localization length is much larger, because it corresponds to the one we would have without mixing multiplied by the number of modes and can therefore exceed the length of the device, if the number of modes is large enough. The effect of magnetic field in terms of mode-mixing and suppression of localization can easily be seen also from the dependence of device resistance as a function of the number of barriers, which crosses over from an exponential to a linear behavior as the value of the magnetic field is increased.

A. Model

The model we adopt for our simulations is rather simple and is based on the application of the recursive Green's function technique [11], [12] for the calculation of the transmission matrix of the overall structure. We consider a series of cascaded barriers with a lateral hard-wall confinement: it is substantially a quantum wire with transverse barriers spaced by an amount that is varied randomly to avoid the resonances that would appear if the barriers were equally spaced. The structure is subdivided into sections, each of which corresponds to either

978-1-4577-0192-4/11/$26.00 ©2011 IEEE

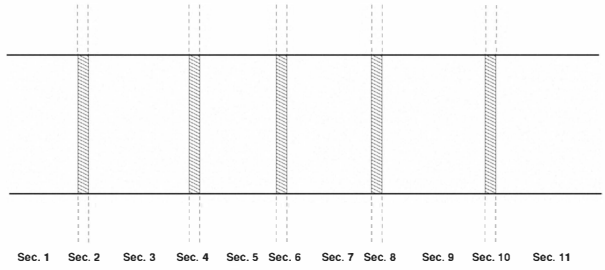

Fig. 1. Layout of a channel with a series of transverse barriers; the structure is divided by the dashed lines into sections with a potential constant along the longitudinal direction.

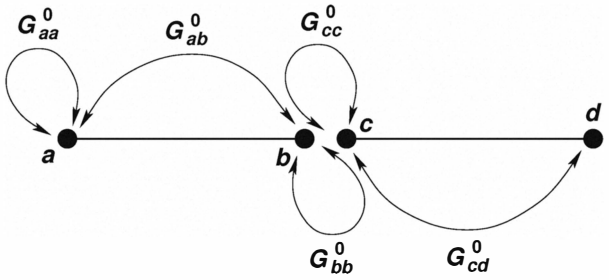

Fig. 2. Schematic representation of two adjacent sections to be joined by means of the Dyson equation: the relevant Green's functions are reported, with a graphic indication of the locations between which they represent the propagation.

a barrier or an interbarrier region (see Fig. 1). Regions of either type are characterized by a potential that is constant in the longitudinal direction, therefore their Green's function matrix (represented, following Refs. [11], [12], in the real space in the longitudinal direction and in mode space along the transverse direction) has a known [13] analytical form. Also the Green's functions of the semiinfinite leads that we assume attached at each end of the device to implement the proper absorbing boundary conditions are available in analytical form. As a result of the longitudinal invariance of the potential within each section, there is no mode mixing, and therefore the matrices representing their Green's functions are diagonal. Then, in order to join the Green's functions for the different sections, we use the Dyson equation, considering the connection between two otherwise separated sections as a perturbation:

$$\langle a|G|d\rangle = \langle a|G^0|d\rangle + \langle a|G^0 V G|d\rangle\,, \tag{1}$$

where G^0 is the unperturbed Green's function, G the Green's function after the application of the perturbation, V is a perturbation matrix, whose elements are given by the overlap integrals between the transverse modes in the facing sections times the "hopping potential" v ($v = -\hbar^2/(2ma^2)$, a being the longitudinal discretization step). The Dyson equation is an implicit equation, but if we represent it over the previously mentioned basis of the modes along the transverse direction and the lattice points along the longitudinal direction, with some algebra [13] we obtain explicit relationships that allow the calculation of the Green's functions of two joined sections from the knowledge of the Green's functions of the uncoupled sections. Let us consider two sections, one spanning from location a to location b, and the other from location c (which is adjacent to b) and location d (see Fig. 2): the Green's function matrices G^0_{aa}, G^0_{ab}, G^0_{bb}, G^0_{cc}, G^0_{cd} for the condition of uncoupled sections are supposed to be known, either from their analytical expressions (if these are simple sections with longitudinally constant potential) or from previous calculations (if they are the result of the combination of multiple elementary sections), and we want to compute G_{aa} and G_{ad} for the situation with coupled sections. These will be the basis for the recursive additions of further sections to the left. The relevant expressions are:

$$G_{aa} = G^0_{aa} + G^0_{ab} V_{bc} \left(I - G^0_{cc} V_{cb} G^0_{bb} V_{bc}\right)^{-1} G^0_{cc} V_{cb} G^0_{ba} \tag{2}$$

$$G_{ad} = Gab^0 V_{bc} \left(I - G^0_{cc} V_{cb} G^0_{bb} V_{bc}\right)^{-1} G^0_{cd} \tag{3}$$

At the end of the recursive procedure we get the Green's function matrix from a location j in the left semiinfinite lead to a location l in the right semiinfinite lead. The transmission matrix between the same locations is obtained using a modified version [11] of the relationships derived by Stone and Szafer [14]:

$$t_{nm} = -i2V(\sin\theta_n \sin\theta_m)^{1/2} e^{i(\theta_m l - \theta_n j)} \langle n|G_{jl}|m\rangle\,, \tag{4}$$

where θ_n (θ_m) is the product of the longitudinal wave vector for the nth (mth) mode at location j (l) by the discretization step a. The exact position of j and l in the leads only affects the phases of the elements of the transmission matrix and therefore has no effect on the conductance and shot noise power spectral densities, which are obtained according to the Landauer [15], [16] and Büttiker [17] expressions, respectively:

$$G = 2\frac{e^2}{h} \sum_{ij} |T_{ij}|^2, \tag{5}$$

where the T_{ij}s are the moduli of the corresponding elements of the transmission matrix t;

$$S_I = 4\frac{e^2}{h} |eV| \mathrm{Tr}\left[t^\dagger t (I - t^\dagger t)\right], \tag{6}$$

where V is the applied voltage bias. This can also be written as

$$S_I = 4\frac{e^2}{h} |eV| \sum_i T_i (1 - T_i), \tag{7}$$

where the T_is are the eigenvalues of the $tt^\dagger$ matrix.

Indeed, in the absence of a magnetic field the problem is just a collection of one-dimensional problems and could be treated in a much simpler fashion, because the transverse modes in the barriers and in the interbarrier regions are identical, the only difference being a translation of the eigenvalues corresponding to the height of the barriers. This implies that the overlap matrices V are diagonal matrices and all the Green's function

matrices are diagonal, too. This also means that, in the absence of a magnetic field, the overall result is not significantly dependent on the number of modes.

The recursive Green's function method becomes however necessary when we turn on the magnetic field, creating an interaction between the different modes, and therefore changing the nature of the problem from 1-dimensional to truly 2-dimensional.

In order to include the effect of the magnetic field, we consider a transverse Landau gauge, yielding a vector potential with a nonzero component only along the transverse direction: $A_y(x_i) = Bx_i$, where x_i is the longitudinal coordinate of the ith slide, and B is the magnetic field (orthogonal to the plane of the device). It has been shown [18] that with such a choice of gauge the transverse wave functions are the same as without magnetic field, with the addition of a Peierls phase factor:

$$\chi_{n,x_i}(y) = \chi^0_{n,x_i}(y)\, e^{-i\frac{e}{\hbar}A_{x_i}y}\,. \tag{8}$$

where $\chi^0_{n,x_i}(y)$ is the $n-$th transverse wave function for the $i-$th section in the absence of magnetic field, $A_{x_i} = Bx_i$ is the the tranverse component of the vector potential, $\hbar$ is the reduced Planck constant.

This makes the inclusion of magnetic field into the recursive Green's function formalism very simple, because we need only to change the way in which the mode overlap matrix V is handled and constructed, since it will now be a complex matrix. Furthermore, for increasing values of the magnetic field, we will need to subdivide each section with a constant longitudinal potential into a number of smaller slices, because a requirement for the proper operation of the method is that each of the transverse slices be threaded only by less than a magnetic field quantum.

In our calculations we consider up to a few thousand slices, which allows us, for a width of the order of 1 micron and a length of a few microns, to handle a magnetic field up to about 1 T. The magnetic field is considered to be constant in the active part of the device, while it is ramped linearly along the leads from zero (at the outer ends) to the value in the active region. The absence of a magnetic field at the outer leads allows us to use Eq.(4) to connect the transmission matrix with the Green's function, a relationship that would not be valid for nonzero local magnetic field.

II. Results

Let us first briefly discuss the results obtained without magnetic field, for a structure characterized by a width of 8 μm and up to 10 barriers.

We treat the effect of finite temperature by averaging over an interval of about 40 μeV around a Fermi level at 9.03 eV from the bottom of the conduction band, corresponding to a typical value for the 2-dimensional electron gas (2DEG) in a GaAs/AlGaAs heterostructure. Consistently, the effective mass is chosen to be 0.067 m_0, the value typical for Gallium Arsenide. The amplitude of the interval over which averaging is performed corresponds to about 10 kT at a temperature of 50 mK, typical of experiments on mesoscopic systems. A bias of 10 kT is usually chosen in shot noise measurements to have a prevalence of the shot noise power spectral density over the thermal noise power spectral density.

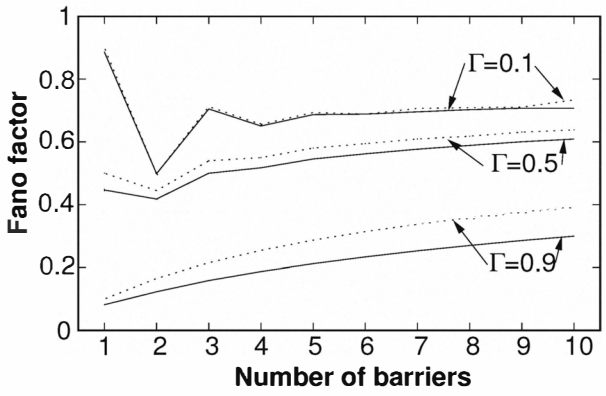

Fig. 3. Fano factor as a function of the number of barriers for three different values of the average barrier transparency; solid curves are for realistic barriers with a dependence of transmission on the longitudinal wave vector, dotted curves are for idealized barriers with constant transmission; all results are obtained averaging over 50 sets of interbarrier distances.

We have also included averaging over different distributions for the interbarrier distances. As previously mentioned, it is necessary to make the interbarrier distances slightly different from each other, in order to avoid resonance phenomena, which would appear otherwise.

This result is achieved by further averaging over 50 different sets of interbarrier distances (with an average value of 3 μm), which can easily be shown to be almost exactly equivalent to introducing a random phase shift for each propagating mode when travelling between two barriers, an approach typically used to phenomenologically model dephasing effects.

The results are shown in Fig. 3: it is possible to see that for the different values of the barrier transparencies used there is no clear trend towards an asymptotic value 1/3 of the Fano factor as the number of barriers is increased. We rather observe that for more opaque barriers the Fano factor is in any case over 1/3 for any barrier number, while for more transparent barriers the Fano factor starts from rather low values and then increases, without however approaching a clear 1/3 limit. For each barrier transparency we report two curves: a solid one corresponding to realistic barriers, for which the transparency is actually not exactly constant, but a function of the longitudinal wave vector and therefore different for the different propagating modes (the reported transparency is an averaged value, over all propagating modes), and a dotted one corresponding to idealized barriers (such as the ones considered in semiclassical models) with a constant transparency, independent of the wave vector. It is apparent that there is no significant qualitative difference between the behaviors of the realistic and of the idealized barriers, therefore this cannot be the reason for the sharp discrepancy between the quantum and the semiclassical models.

The actual issue at the basis of the sharp difference between the results of the two approaches is that the semiclassical

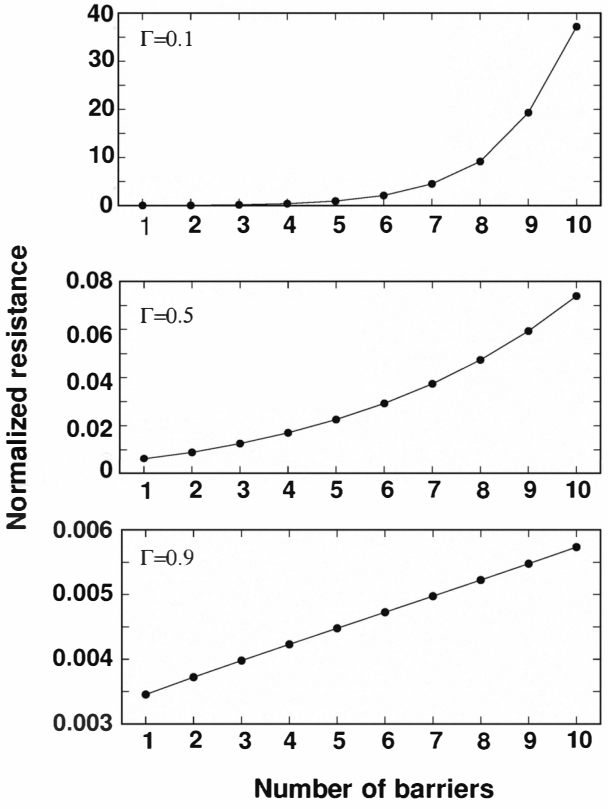

Fig. 4. Normalized (with respect to the inverse of the conductance quantum) resistance as a function of the number of barriers for three different values of the average barrier transparency.

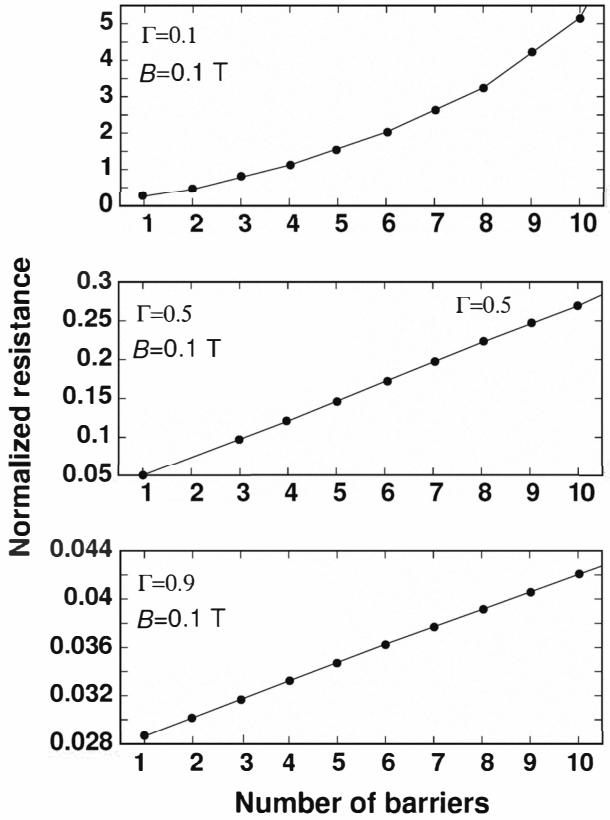

Fig. 5. Normalized (with respect to the inverse of the conductance quantum) resistance as a function of the number of barriers for three different values of the average barrier transparency, in the presence of magnetic field of 0.1 T orthogonal to the plane of the device.

model does not exhibit strong localization, while this appears in the quantum model, due to the phase coherence. In the presence of 1-D disorder, such as the one due to randomly spaced barriers, the localization length is of the order of the mean free path, thereby making it impossible to satisfy the inequality $L \ll D \ll \lambda$, where L is the mean free path, D is the device length, and λ is the localization length. In the case of 2-D and 3-D disorder there is mode mixing, therefore the localization length becomes of order NL [19] (where N is the number of propagating modes) and the inequality can be satisfied for a large enough N. The presence of strong localization can be deduced from the dependence of the resistance on the number of barriers (see Fig. 4): for the less transparent barriers the exponential dependence on the number of barriers is apparent. Dephasing introduced by means of the inclusion of a random phase (as in our calculations) does not remove such localization. Inelastic scattering due to phonons could produce a strong enough scattering, but in the case of significant thermal scattering Johnson-Nyquist noise would prevail in the device. Therefore we expect that in practical experimental structures, such as superlattices or a semiconductor quantum wire with barriers defined by means of transverse depletion gates [20], transport will non achieve the diffusive regime and the Fano factor will not be 1/3.

As mentioned in the introduction, the application of a magnetic field orthogonal to the plane of the device does introduce mode mixing: considering the gauge adopted in the section about the numerical model, the Peierls phase factor makes the wave functions in two adjacent sections different, thereby leading to a nondiagonal V matrix, which implies mode mixing. As a result of mode mixing, the localization length is increased, as can be deduced by the comparison between Fig. 4 and Fig. 5, where the resistance as a function of the number of barriers is reported for the same values of the transparency as in the previous figure, but this time for a 1 μm wide wire and in the presence of an orthogonal magnetic field of 0.1 T. The overall resistance is increased, because of the smaller width and the reduction in the number of propagating modes due to the magnetic field, but we notice that the dependence of the resistance on the number of barriers is now linear for the two larger transparency values, and also for $\Gamma = 0.1$ the exponential behavior is associated with a much larger length constant. On the basis of this effect of the magnetic field, we expect that it will have a significant impact also on the Fano factor [21], bringing it closer to the 1/3 value characteristic of diffusive transport.

We have computed the Fano factor as function of the number of barriers for a 1 μm wide wire with a series of unevenly spaced barriers (the mean interbarrier distance

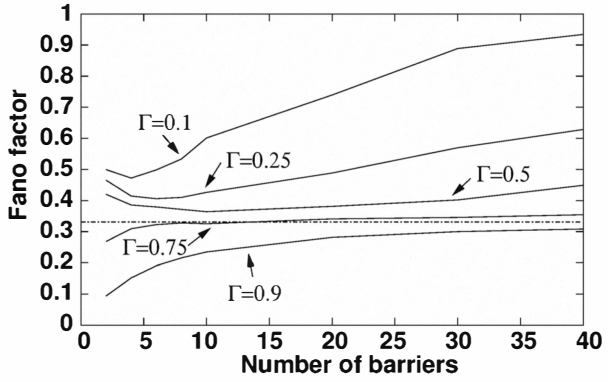

Fig. 6. Fano factor as a function of the number of barriers for a wire 1 μm wide, in the presence of an orthogonal magnetic field of 0.1 T, for a few values of the average barrier transparency.

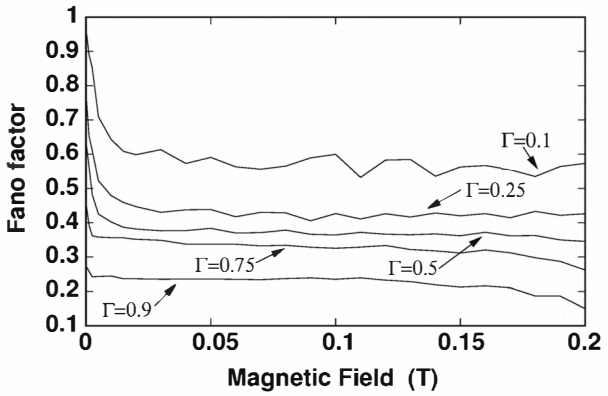

Fig. 7. Fano factor as a function of the orthogonal magnetic field for a wire 1 μm wide with 10 barriers.

is 500 nm) and with a 0.1 T magnetic field orthogonal to the plane of the device. Results are reported in Fig. 6, for a few values of the barrier transparency. It is possible to see that for the two largest values of the transparency the Fano factor approaches the diffusive limit as the number of barriers increases over 25-30. This is because the amount of mode mixing introduced by the magnetic field increases the localization length λ to a value much larger than the mean free path, so that the inequality $L \ll D \ll \lambda$ can be reasonably satisfied. For the case of barriers with lower transparency a much larger number of modes would probably be needed to approach the diffusive limit. In Fig. 7 we report, for the same structure, the dependence of the Fano factor as a function of magnetic field, in the presence of 10 barriers. It is clear that the main dependence on magnetic field is for values below 0.05 T; for higher values we observe a sort of saturation of the effect. With 10 barriers the shot noise suppression factor approaches 1/3 only for a transparency of 0.75, in agreement with the data in Fig. 6.

III. Conclusion

We can conclude that a system of cascaded barriers is in general not characterized, as the number of barriers tends to infinity, by the Fano factor of 1/3 that would be predicted by semiclassical theories. This is the consequence of the fact that localization appears in the presence of 1-D disorder and can be overcome only by some mode-mixing mechanism. One possible such mechanism is that associated with an orthogonal magnetic field, which, by creating interaction among the propagating modes, removes the localization. One could also think of 2-D or 3-D disorder due, for example, to randomly located dopants, but calculations we have performed show that the amount of additional disorder that would be needed is such that it would lead to a diffusive behavior even in the absence of the barriers. Therefore we believe that it is unlikely to observe a suppression of the Fano factor down to 1/3 due to 1-D disorder (i.e. to a series of cascaded barriers). The only experimental data available so far [9] is compatible with this conclusion.

References

[1] C. W. J. Beenakker and M. Büttiker, Phys. Rev. B **46**, 1889 (1992).
[2] Ya. M. Blanter, M. Büttiker, Phys. Rep. **336**, 1 (2000).
[3] W. Schottky, Annalen der Physik **362** 541 (1918).
[4] M. Henny, S. Oberholzer, C. Strunk, and C. Schönenberger, Phys. Rev. B **59**, 2871 (1999).
[5] A. Kolek, A. W. Stadler, and G. Haldaś, Phys. Rev. B **64**, 075202 (2001).
[6] M. Macucci, G. Iannaccone, G. Basso, and B. Pellegrini, Phys. Rev. B **67**, 115339 (2003).
[7] M. J. M. de Jong and C. W. J. Beenakker, Phys. Rev. B **51**, 16867 (1995).
[8] R. Liu, P. Eastman, and Y. Yamamoto, Solid State Commun. **102**, 785 (1997).
[9] W. Song, A. K. M. Newaz, J. K. Son, and E. E. Mendez, Phys. Rev. Lett. **96**, 126803 (2006).
[10] P. Marconcini, M. Macucci, G. Iannaccone, and B. Pellegrini, in the Proceedings of 20th International Conference on Noise and Fluctuations (ICNF 2009), p. 423 (Pisa, Italy, June 2009).
[11] F. Sols, M. Macucci, U. Ravaioli, and Karl Hess, J. Appl. Phys. **66**, 3892 (1989).
[12] M. Macucci, A. Galick and U. Ravaioli, Phys. Rev. B **52**, 5210 (1995).
[13] M. Rieth and W. Schommers (Editors), "Handbook of Theoretical and Computational Nanotechnology," vol. 10, p. 690.
[14] A. D. Stone, A. Szafer, IBM J. Res. Develop. **32**, 384 (1988).
[15] R. Landauer, IBM J. Res. Dev. **1**, 223 (1957).
[16] M. Büttiker, Y. Imry, R. Landauer, S. Pinhas, Phys. Rev. B **31**, 6207 (1985).
[17] M. Büttiker, Phys. Rev. Lett. **65**, 2901 (1990).
[18] M. Governale, D. Boese, Appl. Phys. Lett. **77**, 3215 (2000).
[19] H. Tamura and T. Ando, Phys. Rev. B **44**, 1792 (1991).
[20] M. Totaro, D. Logoteta, P. Marconcini, M. Macucci, R. S. Whitney, Proceedings of the Solid State Device Research Conference, (ESSDERC '09), p. 14 (Athens, Greece, Sept. 2009).
[21] P. Marconcini, M. Macucci, G. Iannaccone, and B. Pellegrini, Phys. Rev. B **79**, 241307(R) (2009).